An Optimal Power Flow Approach to Improve Power System Voltage Stability Using Demand Response

Mengqi Yao, *Student Member, IEEE,* Daniel K. Molzahn, *Member, IEEE,* and Johanna L. Mathieu, *Senior Member, IEEE*

***Abstract*—The increasing penetration of renewables has driven power systems to operate closer to their stability boundaries, increasing the risk of instability. We propose a multiperiod optimal power flow approach that uses demand responsive loads to improve steady-state voltage stability, which is measured by the smallest singular value (SSV) of the power flow Jacobian matrix. In contrast to past work that employs load shedding to improve stability, our approach improves the SSV by decreasing and increasing individual loads while keeping the total loading constant to avoid fluctuation of the system frequency. Additionally, an energy payback period maintains the total energy consumption of each load at its nominal value. The objective function balances SSV improvements against generation costs in the energy payback period. We develop an iterative linear programming algorithm using singular value sensitivities to obtain an AC-feasible solution. We demonstrate its performance on two IEEE test systems. The results show that demand response actions can improve static voltage stability, in some cases more cost-effectively than generation actions. We also compare our algorithm's performance to that of an iterative nonlinear programming algorithm from the literature. We find that our approach is approximately 6 times faster when applied to the IEEE 9-bus system, allowing us to demonstrate its performance on the IEEE 118-bus system.**

***Index Terms*—Demand response, optimal power flow, voltage stability, singular value, iterative linearization.**

NOTATION

Functions

$\mathcal{C}(\cdot)$	Total generation cost
$\mathcal{F}_n^{\mathrm{P}}(\cdot)$	Real power injection at bus n
$\mathcal{F}_n^{\mathrm{Q}}(\cdot)$	Reactive power injection at bus n
$\mathcal{H}_{nm}(\cdot)$	Line flow for line (n,m)
$f_n^{\mathrm{P}}(\cdot)$	Linearization of $\mathcal{F}_n^{\mathrm{P}}$
$f_n^{\mathrm{Q}}(\cdot)$	Linearization of $\mathcal{F}_n^{\mathrm{Q}}$
$h_{nm}(\cdot)$	Linearization of $\mathcal{H}_{nm}$

Sets

$\mathcal{N}$	Set of all buses
$\mathcal{S}_{\mathrm{PV}}$	Set of all PV buses
$\mathcal{S}_{\mathrm{PQ}}$	Set of all PQ buses
$\mathcal{S}_{\mathrm{G}}$	Set of buses with generators
$\mathcal{S}_{\mathrm{DR}}$	Set of buses with responsive loads
$\mathcal{T}$	Set of time periods within optimization problem

This work was supported by NSF Grant ECCS-1549670 and the U.S. DOE, Office of Electricity Delivery and Energy Reliability under contract DE-AC02-06CH11357. M. Yao and J.L. Mathieu are with the Department of Electrical Engineering and Computer Science, University of Michigan, Ann Arbor, MI 48109 USA (e-mail: mqyao@umich.edu, jlmath@umich.edu). D.K. Molzahn is with School of Electrical and Computer Engineering, Georgia Institute of Technology, Atlanta, GA 30313 USA (email: molzahn@gatech.edu).

Variables & Parameters

J	Jacobian matrix
$P_{\mathrm{d},n}$	Real power demand at bus n
$P_{\mathrm{g},n}$	Real power generation at bus n
P_{loss}	Total power loss in the system
$Q_{\mathrm{d},n}$	Reactive power demand at bus n
$Q_{\mathrm{g},n}$	Reactive power generation at bus n
T_t	Length of time period t
u	Left singular vector
V_n	Voltage magnitude at bus n
w	Right singular vector
α	Weighting factor
ε	Loss management strategy parameter
θ_n	Voltage angle at bus n
λ	Eigenvalue of a matrix
μ_n	Ratio between reactive and real demand at bus n
σ	Singular value of a matrix
σ_0	Smallest singular value of a matrix
Σ, U, W	Singular Value Decomposition (SVD) matrices
χ	Operating point

Bold symbols denote vectors including all variables of a type. Overlines and underlines represent the upper and lower limits for variables. Numbers in the parentheses $(\cdot)$ refer to the period number. Subscript 'ref' denotes the slack bus. Superscript '$*$' denotes the current value of a variable and superscript 'T' denotes the transpose of a matrix. The notation $X \succeq 0$ means that X is a positive semidefinite matrix. For notational simplicity, we assume that each bus has at most one generator and at most one load.

I. INTRODUCTION

INCREASING penetrations of renewable energy sources can negatively impact power systems stability [1], [2]. Specifically, power-electronics-connected fluctuating renewable generation from wind and solar introduce more variability in operating points, reduce system inertia, and decrease the controllability of active power injections. A variety of methods have been proposed to improve power system stability margins including generation dispatch [3], locating/sizing distributed generation [4], and use of advanced power electronic devices [5]. Demand Response (DR) can also be used to improve power system stability. For example, [6]–[8] propose methods to coordinate loads to help balance supply and demand, improving frequency stability. As we increase the controllability of distributed electric loads to enable their participation in a variety of DR programs and electricity markets [9], we also unleash their potential to provide a variety of stability-related services not typically rewarded in existing programs or markets. A key research question is whether loads are effective at improving stability margins other than those related to frequency stability, for example, voltage or rotor angle stability margins. However, harnessing loads for these purposes requires the development of new algorithms, the design of which influences their effectiveness.

In this paper, we propose a multiperiod optimal power flow (OPF) approach that uses DR to improve steady-state voltage stability. In contrast to past work that developed load shedding approaches to improve voltage stability [10]–[12], we decrease and increase loads while keeping the total loading constant to avoid fluctuation of the system frequency, and we "pay back" the changes to each load so its total energy consumption is unchanged. We envision that such an approach would be used only occasionally, when voltage stability margins are below those desired, but not so small that emergency actions are immediately necessary. DR actions could be executed quickly while ramp-rate-limited generators begin to respond, eventually relieving the loads. Beyond developing the problem formulation and solution algorithm, our objective is to compare the stability margin improvement and cost of load actions to those of generator actions in order to understand both the advantages and disadvantages of the approach. Additionally, we compute the amount of load shedding that would be necessary to achieve the same stability margin improvements as load shifting.

Steady-state voltage stability margins estimate how far an operating point is from instability due to voltage collapse. Various margins have been proposed, including the loading margin, which is the distance between the current operating point and the maximum loading point [3]. The loading margin is calculated using continuation power flow methods, where the load and generation are usually increased uniformly (in a multiplicative sense) throughout the system [13], [14]. A drawback of this method is that it assumes a single direction of changes in power injections. In [15], we use DR to maximize the loading margin and compare the results to those generated with an earlier version of the approach proposed in this paper. Another margin is the distance to the closest saddle-node bifurcation (SNB) point. References [16], [17] derive a system of nonlinear equations from which we can calculate the optimal control direction, which is antiparallel to the normal vector at the closest SNB. However, changing the loads in this direction may change the total loading. In [18] we pose an optimization problem that uses DR to maximize the distance to the closest SNB. However, we cannot guarantee that we will find the globally closest SNB and so the algorithm might push the system away from a locally closest SNB and towards the globally closest SNB, thus actually reducing the stability margin. A third margin, which we use in this paper, is the smallest singular value (SSV) of the power flow Jacobian matrix [11], [19]–[25].

The SSV gives us a measure of how close the Jacobian is to being singular, i.e., power flow infeasibility. Feasibility and stability are closely linked [26]. The advantages of using the SSV as a voltage stability margin are that 1) it captures any direction of changes in power injections and 2) there exist approximate mathematical formulations suitable for inclusion in optimization problems, e.g., [11], [27], [28]. It is simpler to work with than the distance to the closest SNB because there is only one SSV, while there can be a large number of locally closest SNBs. The disadvantages of using the SSV are that 1) it only provides implicit information on the distance to the solvability boundary, 2) it does not capture the impact of all engineering constraints (e.g., reactive power limits could be reached prior to power flow singularity [29]), and 3) it may not be well-behaved, specifically, [30] found that the SSV at voltage collapse varies significantly as function of the loading direction (see Fig. 3 of [30]). Additionally, 4) its numerical value is system-dependent [24] and so the threshold value for a particular system would need to be determined from operator experience. Moreover, 5) the nonlinear programming (NLP) algorithm for solving approximate mathematical formulation [28] does not scale to realistically-sized system. Despite these issues, we base our approach on the SSV in order to exploit the approximate mathematical formulation [27], [28] and we develop an improved solution algorithm that scales significantly better. Recognizing the potential advantages of other stability margins, our ongoing work is exploring the development of analogous formulations based on other stability margins.

The contributions of this paper are four-fold. 1) We formulate a multiperiod optimal power flow problem that uses spatio-temporal load shifting to improve voltage stability. In the first period, we maximize the SSV of the power flow Jacobian by changing the loading pattern subject to the AC power flow equations, engineering limits, and a constraint that forces the total loading to be constant. The second period minimizes the generation cost while paying back energy to each load and maintaining the SSV. 2) We develop a computationally-tractable iterative linear programming (LP) solution algorithm using singular value sensitivities [11], [12], [31] and benchmark it against the NLP algorithm in [28]. 3) We conduct case studies using the IEEE 9- and 118-bus systems to determine optimal loading patterns and assess algorithmic performance. 4) We compare the cost and performance of spatio-temporal load shifting to that of generator actions and load shedding.

This paper builds on our preliminary work [15], which developed a single-period formulation that uses DR to maximize the SSV, but does not consider energy payback. We proposed an iterative LP solution algorithm using eigenvalue sensitivities; however, our new algorithm in this paper is far more computationally tractable, as we will show, allowing us to demonstrate scalability to the IEEE 118-bus system.

The remainder of the paper is organized as follows. Section II describes the problem and our assumptions. Section III presents the formulation and solution algorithm. Section IV shows the results of our case studies and Section V concludes.

II. Problem Description & Assumptions

A conceptual illustration of the problem is shown in Fig. 1. The system is initially operating with an adequate stability

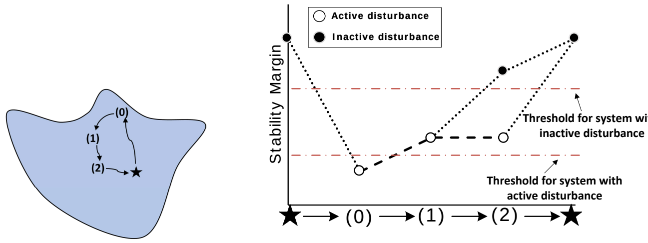

(a) (b)

Fig. 1. Conceptual illustration of the problem. The blue area (left) is the feasibility/stability region of the power system. The operating point moves from the star (pre-disturbance) to Operating Point 0 (post-disturbance) to Operating Point 1 (DR action) to Operating Point 2 (energy payback) and back to the star. The change in stability margin is shown on the right, with two options for Operating Point 2 based on whether or not the disturbance is still active.

margin at an operating point (star) determined via unit commitment and economic dispatch. A disturbance happens (e.g., a line goes out of service) causing the operating point to move towards the feasibility/stability boundary (i.e., to Operating Point 0) and the stability margin to drop to a point below the stability threshold corresponding to the current system topology (i.e., "threshold for system with active disturbance" shown in the figure). Note that SSVs computed for systems with different topologies are incomparable since the Jacobian changes. This means we cannot compare the SSVs denoted with black circles to those denoted with white circles. Additionally, the system operator would need to determine a stability threshold for each post-disturbance topology.

When the SSV is below its stability threshold, because slight variations in power injections might cause the operating point to leave the stable operating region. The system operator dispatches quick-acting resources including DR to maximize the stability margin (Operating Point 1). After a short period of time, the system operator determines the minimum cost dispatch of slower-acting generators that relieves the loads, pays back the changes made to each load at Operating Point 1, and maintains/improves the stability margin (Operating Point 2). The payback sets the energy consumed by each load while at Operating Point 2 to its nominal (i.e., baseline) consumption plus/minus the energy not consumed/consumed while at Operating Point 1. As shown in Fig. 1(b), at Operating Point 2, the achievable stability margin and associated stability threshold is a function of whether or not the disturbance is still active. When it is no longer active and the energy is paid back, the system returns to its initial operating point, or another point with an adequate stability margin.

Our goal is to determine the optimal dispatches corresponding to Operating Points 1 and 2. Note that we neglect the transition; the path the system takes depends upon how the DR actions are implemented. We pose the problem as a multiperiod optimal power flow problem in which the objective is to minimize a weighted combination of the negative of the stability margin in Period 1 (corresponding to Operating Point 1) and the generation cost in Period 2 (corresponding to Operating Point 2). In each time period, we require the total loading to remain unchanged, so as not to affect the system frequency. We assume that the load at certain buses can be decreased or increased within known limits for a short period of time. For example, the responsive loads could be aggregations of heating and cooling loads, such as commercial building heating, ventilation, and air conditioning (HVAC) systems and residential thermostatically controlled loads (TCLs), e.g., air conditioners and refrigerators that cycle on/off within a temperature dead-band. Increases and decreases in load can be achieved through temperature set point adjustments and/or commands to switch TCLs on/off [9]. These types of loads are flexible in their instantaneous power consumption, but energy constrained (i.e., they must consume a certain amount of energy over time), like energy storage units.

In our base case, we use loads alone to improve the stability margin in Period 1. Generator real power injections are held constant with the exception of that associated with the slack bus, which compensates for the small change in system losses resulting from the change in loading pattern. (Note we could have alternatively assumed a distributed slack formulation.) Generator reactive power injections adjust to maintain voltage magnitudes at the PV buses. We model all loads as constant real power loads with constant power factor. As shown in [32], our approach is fully extendable to inclusion of a variety of other load models, including ZIP load and induction motor models.

Beyond our base case, we also investigate cases in which we allow (ramp-rate-limited) generator real power injections and voltage magnitudes at PV buses to change in Period 1. We also explore an alternative loss management strategy in which we require the total loading *plus system losses* to remain unchanged so that no generator (including the slack bus) is required to respond in Period 1. The mathematical formulation is provided in the next section.

Since we focus on static voltage stability, we ignore power system dynamics. Investigating the dynamic stability implications of changes in operating points is a subject for future research.

III. Optimization Approach

This section first formulates our nonconvex nonlinear multiperiod optimization problem. We then describe some approaches that have been proposed to solve similar problems in the past. Finally, we present our iterative LP algorithm based on singular value sensitivities.

A. Multiperiod Optimal Power Flow Problem

Let $\mathcal{T} = \{1, 2\}$ be the set of time periods within the optimization problem, T_1 be the length of Period 1, and T_2 be the length of Period 2. Lengths T_1 and T_2 are not necessarily equal, as shown in Fig. 2. For notational simplicity, we assume the real power demand at bus n, $P_{\mathrm{d},n}(t)$, is constant within a time period and the nominal real power demand in all periods is equal to $P_{\mathrm{d},n}(0)$; however, the formulation could be easily extended to incorporate time-varying demands.

Let $\mathcal{N}$ be the set of all buses, $\mathcal{S}_{\mathrm{PV}}$ be the set of all PV buses, and $\mathcal{S}_{\mathrm{PQ}}$ be the set of all PQ buses. Additionally, let $\mathcal{S}_{\mathrm{G}}$ be the set of all buses with generators, i.e., all PV buses in addition to the slack bus, and let $\mathcal{S}_{\mathrm{DR}}$ be the set of buses

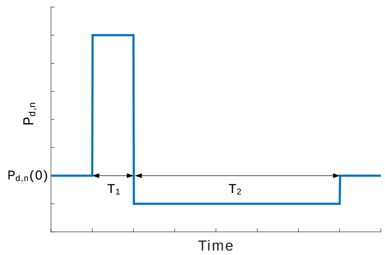

Fig. 2. Example dispatched demand $P_{\mathrm{d},n}$ at bus n in Periods 1 and 2, where $P_{\mathrm{d},n}(0)$ is its nominal demand. The total energy consumed over both periods is equal to its nominal consumption.

with responsive loads; the buses comprising $\mathcal{S}_{\mathrm{DR}}$ may be PV or PQ buses. In our case studies, we assume that a portion of the existing loads in the network are responsive.

The multiperiod optimal power flow problem determines the operating points in each time period that balance the two objectives: maximizing the SSV of the power flow Jacobian matrix in Period 1 and minimizing the generation cost in Period 2. The general formulation is as follows.

$$\min_{\substack{\boldsymbol{P}_{\mathbf{g}}(t),\boldsymbol{Q}_{\mathbf{g}}(t),\\ \boldsymbol{P}_{\mathbf{d}}(t),\boldsymbol{Q}_{\mathbf{d}}(t),\\ \boldsymbol{V}(t),\boldsymbol{\theta}(t),\sigma_0(t)}} \quad -\alpha\sigma_0(1) + \mathcal{C}(\boldsymbol{P}_{\mathbf{g}}(2)) \tag{1a}$$

s.t. $\quad (\forall t \in \mathcal{T})$

$$\sigma_0(t) = \sigma_{\min}\{J(\boldsymbol{\theta}(t), \boldsymbol{V}(t))\} \tag{1b}$$

$$\mathcal{F}_n^{\mathrm{P}}(\boldsymbol{\theta}(t), \boldsymbol{V}(t)) = P_{\mathrm{g},n}(t) - P_{\mathrm{d},n}(t) \qquad \forall n \in \mathcal{N} \tag{1c}$$

$$\mathcal{F}_n^{\mathrm{Q}}(\boldsymbol{\theta}(t), \boldsymbol{V}(t)) = Q_{\mathrm{g},n}(t) - Q_{\mathrm{d},n}(t) \qquad \forall n \in \mathcal{N} \tag{1d}$$

$$\sum_{n\in\mathcal{S}_{\mathrm{DR}}} P_{\mathrm{d},n}(1) = \sum_{n\in\mathcal{S}_{\mathrm{DR}}} P_{\mathrm{d},n}(0) + \varepsilon\left(P_{\mathrm{loss}}(0) - P_{\mathrm{loss}}(1)\right) \tag{1e}$$

$$T_1 P_{\mathrm{d},n}(1) + T_2 P_{\mathrm{d},n}(2) = (T_1 + T_2) P_{\mathrm{d},n}(0) \ \ \forall n \in \mathcal{S}_{\mathrm{DR}} \tag{1f}$$

$$P_{\mathrm{d},n}(t) \cdot \mu_n = Q_{\mathrm{d},n}(t) \qquad \forall n \in \mathcal{N} \tag{1g}$$

$$P_{\mathrm{d},n}(t) = P_{\mathrm{d},n}(0) \qquad \forall n \in \mathcal{N} \setminus \mathcal{S}_{\mathrm{DR}} \tag{1h}$$

$$\theta_{\mathrm{ref}}(t) = 0 \tag{1i}$$

$$\sigma_0(2) \geq \sigma_0(1) \tag{1j}$$

$$\mathcal{H}_{nm}(\boldsymbol{\theta}(t), \boldsymbol{V}(t)) \leq \overline{\mathcal{H}}_{nm} \tag{1k}$$

$$\mathcal{H}_{mn}(\boldsymbol{\theta}(t), \boldsymbol{V}(t)) \leq \overline{\mathcal{H}}_{mn} \tag{1l}$$

$$\underline{P}_{\mathrm{g},n}(t) \leq P_{\mathrm{g},n}(t) \leq \overline{P}_{\mathrm{g},n}(t) \qquad \forall n \in \mathcal{S}_{\mathrm{G}} \tag{1m}$$

$$\underline{Q}_{\mathrm{g},n}(t) \leq Q_{\mathrm{g},n}(t) \leq \overline{Q}_{\mathrm{g},n}(t) \qquad \forall n \in \mathcal{S}_{\mathrm{G}} \tag{1n}$$

$$\underline{P}_{\mathrm{d},n}(t) \leq P_{\mathrm{d},n}(t) \leq \overline{P}_{\mathrm{d},n}(t) \qquad \forall n \in \mathcal{S}_{\mathrm{DR}} \tag{1o}$$

$$\underline{V}_n(t) \leq V_n(t) \leq \overline{V}_n(t) \qquad \forall n \in \mathcal{N} \tag{1p}$$

The cost function is a linear combination of the SSV σ_0 of the power flow Jacobian matrix $J(\boldsymbol{\theta}, \boldsymbol{V})$ in Period 1 and the generation cost $\mathcal{C}(\cdot)$ in Period 2, where $\alpha \geq 0$ is a weighting factor. Constraint (1b) defines the SSV of $J(\boldsymbol{\theta}, \boldsymbol{V})$ where $\sigma_{\min}$ is a function that takes the SSV of a matrix. Constraints (1c) and (1d) are the nonlinear AC power flow equations [33]. Constraint (1e) sets the total system load in Period 1 to be equal its nominal value plus a portion of the change in system losses, where the real power loss is $P_{\mathrm{loss}}(t) = \sum_{n\in\mathcal{N}}(P_{\mathrm{g},n}(t) - P_{\mathrm{d},n}(t))$ and ε is a parameter that defines the loss management strategy (i.e., $0 \leq \varepsilon \leq 1$, where $\varepsilon = 1$ allocates loss management exclusively to the loads, while $\varepsilon = 0$ allocates loss management exclusively to the slack bus). Constraint (1f) enforces energy payback, specifically, that the energy consumed over both periods by each load is equal to its nominal consumption. Constraint (1g) fixes the power factor of each load, where μ_n is the ratio between the reactive and real demand at bus n. Constraint (1h) fixes the non-responsive demand to its nominal value. Constraint (1i) sets the slack bus voltage angle. Constraint (1j) ensures that the SSV in Period 2 is greater than or equal to that in Period 1. Constraints (1k)–(1p) limit the line flows, real and reactive power generation at generator buses, real power demand at buses with responsive loads, and voltage magnitudes at all buses. The real power generation limits $\left(\underline{P}_{\mathrm{g},n}(t), \overline{P}_{\mathrm{g},n}(t)\right)$ depend on whether or not the generator is modeled as responsive in t, its minimum/maximum output, its ramp limits, and, for the slack bus, the loss management strategy (i.e., when $\varepsilon = 0$ the slack bus real power generation will be allowed to vary, but when $\varepsilon = 1$ it will be fixed). The real power demand limits $\left(\underline{P}_{\mathrm{d},n}(t), \overline{P}_{\mathrm{d},n}(t)\right)$ depend on the flexibility of the responsive loads. The voltage limits $\left(\underline{V}_n(t), \overline{V}_n(t)\right)$ depend on whether or not the generator voltages are allowed to adjust in period t.

In our base case, the slack bus manages the change in losses, (i.e., $\varepsilon = 0$) but the real power generation of all other generators is fixed in Period 1. Additionally, voltage magnitudes at all generator buses are fixed in Period 1. Specifically,

$$\begin{aligned} &P_{\mathrm{g},n}(1) = P_{\mathrm{g},n}(0) && \forall n \in \mathcal{S}_{\mathrm{PV}} \\ &\underline{P}_{\mathrm{g,ref}}(1) \leq P_{\mathrm{g,ref}}(1) \leq \overline{P}_{\mathrm{g,ref}}(1) && \\ &V_n(1) = V_n(0) && \forall n \in \mathcal{S}_{\mathrm{G}} \\ &\underline{V}_n(1) \leq V_n(1) \leq \overline{V}_n(1) && \forall n \in \mathcal{S}_{\mathrm{PQ}} \end{aligned}$$

In Period 2, generator real power generation and voltage magnitudes are allowed to change within their limits, specifically,

$$\begin{aligned} &\underline{P}_{\mathrm{g},n}(2) \leq P_{\mathrm{g},n}(2) \leq \overline{P}_{\mathrm{g},n}(2) && \forall n \in \mathcal{S}_{\mathrm{G}} \\ &\underline{V}_n(2) \leq V_n(2) \leq \overline{V}_n(2) && \forall n \in \mathcal{N} \end{aligned}$$

We investigate seven additional cases in which we vary the decision variables that are allowed to change in Period 1 (specifically, $P_{\mathrm{g,ref}}$, $P_{\mathrm{g},n}\, \forall n \in \mathcal{S}_{\mathrm{PV}}$, $V_n\, \forall n \in \mathcal{S}_{\mathrm{G}}$, and $P_{\mathrm{d},n}, Q_{\mathrm{d},n}\, \forall n \in \mathcal{S}_{\mathrm{DR}}$), the loss management strategy, and, for cases in which generator real power generation is allowed to change in Period 1, whether or not we impose a ramp rate. The cases and associated results, which will be discussed later, are summarized in Table I.

The difficulty in solving (1) stems from the existence of the implicit constraint (1b). Because the singular values of a matrix A are the square roots of the eigenvalues of A^TA, we can replace (1b) with

$$J(t)^T J(t) - \lambda_0(t) I \succeq 0 \tag{2}$$

$$\sigma_0(t) = \sqrt{\lambda_0(t)} \tag{3}$$

where the semidefinite constraint (2) forces λ_0 to be the smallest eigenvalue of $J(t)^T J(t)$, I is an identity matrix of appropriate size, and we have simplified the expression for the power flow Jacobian matrix for clarity. The SSV of $J(t)$ is the square root of λ_0, as shown in (3).

B. Existing Solution Approaches

A variety of methods have been used to solve problems similar to (1). For example, [34] computes the Hessian of (1b) and then applies an Interior Point Method to solve the nonlinear optimization problem. However, computation of the second derivatives of singular values is computationally difficult. Specifically, in [34], they are obtained through numerical analysis by applying small perturbations to the operating point. Alternatively, since (2) is a semidefinite constraint, we could use semidefinite programming (SDP) by applying a semidefinite relaxation of the AC power flow equations [35], [36]. However, if the relaxation is not tight at the optimal solution, the solution will not be the optimal solution of (1) and, moreover, it will not be feasible.

In this section, we develop a new solution approach that overcomes the drawbacks of the aforementioned approaches. Specifically, our approach uses the first derivatives of singular values obtained using singular value sensitivities, reducing the necessary computation as compared to the second-order method in [34]. We also include the full nonlinear AC power flow equations and solve the resulting optimization problem via an iterative LP algorithm in which 1) the objective function and constraints are linearized such that we can compute a step in the optimal direction using LP, 2) the AC power flow equations are solved for the new operating point (i.e., the original operating point plus the optimal step), and 3) the process is repeated until convergence. Iterative LP [33, p. 371] is commonly used to solve various optimal power flow problems, e.g., [15], [32], [33], [37].

Our approach is an extension of the iterative NLP approach proposed in [28], which we will now describe. It takes advantage of the Singular Value Decomposition (SVD) of the Jacobian, i.e.,

$$J(t) = U(t)\Sigma(t)W(t)^T, \tag{4}$$

where $\Sigma(t)$ is a diagonal matrix, $U(t)$ and $W(t)$ are orthogonal singular vector matrices (i.e., $U(t)U(t)^T = I, W(t)W(t)^T = I$). Around a given operating point, the approximate SSV of $J(t)$ is [28]

$$\widetilde{\sigma}_0(t) = u_0(t)^T J(t) w_0(t), \tag{5}$$

where $u_0(t), w_0(t)$ are the corresponding left and right singular vectors.

Since implicit constraint (1b) can be approximated by (5), we can write our problem as a nonlinear optimization problem

$$\min_{\substack{\boldsymbol{P}_{\mathbf{g}}(t),\boldsymbol{Q}_{\mathbf{g}}(t),\\ \boldsymbol{P}_{\mathbf{d}}(t),\boldsymbol{Q}_{\mathbf{d}}(t),\\ \boldsymbol{V}(t),\boldsymbol{\theta}(t),\widetilde{\sigma}_0(t)}} -\alpha\widetilde{\sigma}_0(1) + \mathcal{C}(\boldsymbol{P}_{\mathbf{g}}(2)) \tag{6a}$$

$$\text{s.t} \quad (\forall t \in \mathcal{T}) \quad \text{constraints (1c)–(1p)}, (5) \tag{6b}$$

To obtain the solution to our original problem (1), we solve (6), recompute $u_0(t)$ and $w_0(t)$ at the new operating point, and repeat the process until convergence. However, the symbolic matrix multiplication in (5) is complex for large systems. Moreover, each iteration requires solving a nonlinear optimization problem. Therefore, the approach does not scale to realistically-sized power systems, as shown in our case study.

C. New Solution Approach: Iterative Linear Programming using SSV Sensitivities

Our new solution approach uses iterative linear programming where the power flow equations are iteratively linearized around new operating points as in [33, p. 371] and the SSV constraint (5) is linearized using singular value sensitivities. Specifically, the change in the i^{th} singular value of a generic matrix A due to a small perturbation in the operating point χ is [22]

$$\Delta\sigma_i \approx \sum_k u_i^T \frac{\partial A}{\partial \chi_k}\bigg|_{\chi^*} w_i \Delta\chi_k, \tag{7}$$

where k indexes χ and χ^* is the current operating point. Therefore, the sensitivity of the SSV of $J(t)$ is

$$\Delta\sigma_0 \approx \sum_{n\in\{\mathcal{S}_{\text{PV}},\mathcal{S}_{\text{PQ}}\}} \left[u_0^T \frac{\partial J}{\partial \theta_n} w_0\right] \Delta\theta_n + \sum_{n\in\mathcal{S}_{\text{PQ}}} \left[u_0^T \frac{\partial J}{\partial V_n} w_0\right] \Delta V_n, \tag{8}$$

where we have suppressed the time dependence of each variable for clarity. Note that our previous work [15], [32] used eigenvalue sensitivities, which required computing $J^T J$ and therefore was less scalable.

The resulting linear program solved in each iteration of the iterative LP algorithm is as follows.

$$\min_{\substack{\boldsymbol{\Delta P_{\mathbf{g}}}(t),\boldsymbol{\Delta Q_{\mathbf{g}}}(t),\\ \boldsymbol{\Delta P_{\mathbf{d}}}(t),\boldsymbol{\Delta Q_{\mathbf{d}}}(t),\\ \boldsymbol{\Delta V}(t),\boldsymbol{\Delta\theta}(t),\Delta\sigma_0(t)}} -\alpha\Delta\sigma_0(1) + \sum_{n\in\mathcal{S}_{\text{G}}} \frac{\partial\mathcal{C}(\boldsymbol{P}_{\mathbf{g}}(2))}{\partial P_{\text{g},n}(2)}\bigg|_{\boldsymbol{P}_{\text{g}}^{*}(2)} \Delta P_{\text{g},n}(2) \tag{9a}$$

s.t. $\quad (\forall t \in \mathcal{T})$

$$\Delta\sigma_0(t) = \sum_{n\in\{\mathcal{S}_{\text{PV}},\mathcal{S}_{\text{PQ}}\}} \left[u_0(t)^T \frac{\partial J(t)}{\partial \theta_n} w_0(t)\right] \Delta\theta_n(t) + \sum_{n\in\mathcal{S}_{\text{PQ}}} \left[u_0(t)^T \frac{\partial J(t)}{\partial V_n} w_0(t)\right] \Delta V_n(t) \tag{9b}$$

$$f_n^{\text{P}}(\boldsymbol{\Delta\theta}(t), \boldsymbol{\Delta V}(t)) = \Delta P_{\text{g},n}(t) - \Delta P_{\text{d},n}(t) \quad \forall n \in \mathcal{N} \tag{9c}$$

$$f_n^{\text{Q}}(\boldsymbol{\Delta\theta}(t), \boldsymbol{\Delta V}(t)) = \Delta Q_{\text{g},n}(t) - \Delta Q_{\text{d},n}(t) \quad \forall n \in \mathcal{N} \tag{9d}$$

$$\sum_{n\in\mathcal{S}_{\text{DR}}} \Delta P_{\text{d},n}(1) = -\varepsilon\Delta P_{\text{loss}}(1) \tag{9e}$$

$$T_1\Delta P_{\text{d},n}(1) + T_2\Delta P_{\text{d},n}(2) = 0 \quad \forall n \in \mathcal{S}_{\text{DR}} \tag{9f}$$

$$\Delta P_{\text{d},n}(t)\cdot\mu_n = \Delta Q_{\text{d},n}(t) \quad \forall n \in \mathcal{N} \tag{9g}$$

$$\Delta P_{\text{d},n}(t) = 0 \quad \forall n \in \mathcal{N}\setminus\mathcal{S}_{\text{DR}} \tag{9h}$$

$$\Delta\theta_{\text{ref}}(t) = 0 \tag{9i}$$

$$\sigma_0^*(2) + \Delta\sigma_0(2) \ge \sigma_0^*(1) + \Delta\sigma_0(1) \tag{9j}$$

$$h_{nm}(\boldsymbol{\Delta\theta}(t), \boldsymbol{\Delta V}(t)) \le \overline{h}_{nm} \tag{9k}$$

$$h_{mn}(\boldsymbol{\Delta\theta}(t), \boldsymbol{\Delta V}(t)) \le \overline{h}_{mn} \tag{9l}$$

$$\underline{P}_{\text{g},n}(t) \le P_{\text{g},n}^*(t) + \Delta P_{\text{g},n}(t) \le \overline{P}_{\text{g},n}(t) \quad \forall n \in \mathcal{S}_{\text{G}} \tag{9m}$$

$$\underline{Q}_{\text{g},n}(t) \le Q_{\text{g},n}^*(t) + \Delta Q_{\text{g},n}(t) \le \overline{Q}_{\text{g},n}(t) \quad \forall n \in \mathcal{S}_{\text{G}} \tag{9n}$$

$$\underline{P}_{\text{d},n}(t) \le P_{\text{d},n}^*(t) + \Delta P_{\text{d},n}(t) \le \overline{P}_{\text{d},n}(t) \quad \forall n \in \mathcal{S}_{\text{DR}} \tag{9o}$$

$$\underline{V}_n(t) \le V_n^*(t) + \Delta V_n(t) \le \overline{V}_n(t) \quad \forall n \in \mathcal{N} \tag{9p}$$

$$\Delta\sigma_0(t) \le \overline{\Delta\sigma_0}, \tag{9q}$$

where (9b) is the linearized SSV constraint and (9c)–(9p) correspond to (1c)–(1p), where $\Delta P_{\text{loss}}(t) = \sum_{n\in\mathcal{N}}(\Delta P_{\text{g},n}(t) -$

$\Delta P_{\mathrm{d},n}(t)$) and superscript '*' denotes the current value of a variable. Constraint (9q) limits the change in $\Delta\sigma_0(t)$ since the linearizations are only valid near the current operating point.

The solution algorithm is given in Algorithm 1. We initialize the operating points of Periods 1 and 2, $\chi^*(1), \chi^*(2)$, at the operating point of Period 0, $\chi(0)$. Then, we compute the constraints of (9) at the current values of the operating points and solve (9) to obtain the optimal change in operating point $\Delta\chi^{\mathrm{opt}}(t)\,\forall t \in \mathcal{T}$. We use those changes to compute updated operating point estimates $\chi'(t)\,\forall t \in \mathcal{T}$. However, in general, $\chi'(t)\,\forall t \in \mathcal{T}$ will not be feasible in the AC power flow equations. Therefore, we solve the AC power flow equations for each time period using components of $\chi'(t)$, specifically, $\boldsymbol{P}_{\mathrm{g}}, \boldsymbol{P}_{\mathrm{d}}, \boldsymbol{Q}_{\mathrm{d}}$, and $V_n\,\forall n \in \mathcal{S}_{\mathrm{G}}$, to obtain the new values of the operating points, $\chi^*(1), \chi^*(2)$. We use these values to compute the new values of the SSVs, $\sigma_0^*(t)\,\forall t \in \mathcal{T}$, and the value of the objective function in (9a). We repeat the process until the absolute value of the objective function in (9a) is less than a threshold (here, 10^{-5}), and the outputs are the final operating points and SSVs.

Algorithm 1 Iterative LP using SSV Sensitivities

Input: The operating point of Period 0, $\chi(0)$.

$\chi^*(1) = \chi^*(2) = \chi(0)$.
repeat
  Compute (9b)–(9q) at $\chi^*(1), \chi^*(2)$.
  Solve (9) at $\chi^*(1), \chi^*(2)$ to obtain $\Delta\chi^{\mathrm{opt}}(t)\,\forall t \in \mathcal{T}$.
  $\chi'(t) = \chi^*(t) + \Delta\chi^{\mathrm{opt}}(t)\,\forall t \in \mathcal{T}$.
  Use $\chi'(t)\,\forall t \in \mathcal{T}$ to solve AC power flows to obtain a new $\chi^*(1)$ and $\chi^*(2)$.
  Use $\chi^*(1)$ and $\chi^*(2)$ to calculate $\sigma_0^*(t)\,\forall t \in \mathcal{T}$ and the objective function in (9a).
until the absolute value of the objective function in (9a) is less than 10^{-5}.

Output: $\chi^*(t)\,\forall t \in \mathcal{T}$, $\sigma_0^*(t)\,\forall t \in \mathcal{T}$.

IV. Results

In this section, we conduct a number of case studies using the IEEE 9- and 118-bus systems. Additionally, we compare the SSV improvement achievable in our base case against those of seven additional cases and compare the performance of our iterative LP (ILP) algorithm against the iterative NLP (INLP) algorithm from [28]. Each iteration of the nonlinear optimization problem (6) is solved with `fmincon` in MATLAB.

For all case studies, we use the system data from Matpower [38] and set $\overline{\Delta\sigma_0} = 0.01$. We model the entire load at a bus with responsive demand as flexible, i.e., $0 \leq P_{\mathrm{d},n} \leq 2P_{\mathrm{d},n}(0)\,\forall n \in \mathcal{S}_{\mathrm{DR}}$ in order to get a sense for the maximum achievable change in SSV due to DR. In practice, only a fraction of the load at a particular bus will be responsive. We set $T_1 = 5$ min and choose T_2 as the minimum multiple of 5 min that achieves a feasible solution, though in practice T_1 and T_2 would be a function of the response time of the generators and the flexibility of the loads.

For the IEEE 9-bus system, we assume the system is initially operating at the optimal power flow solution at $5297/hour. A

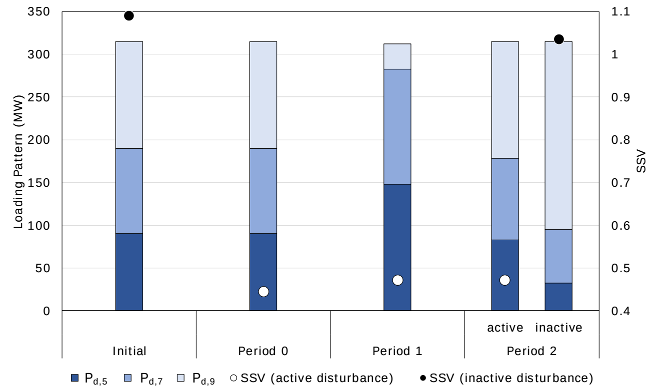

Fig. 3. Loading pattern and SSV in each period for the IEEE 9-bus system.

disturbance takes line 4-9 out of service and the SSV drops to 0.4445, which we assume is below the stability margin threshold. We assume all load is responsive and set $\alpha = 10000$ to prioritize SSV improvement. The effect of the choice of α will be described in the next subsection. If the disturbance is active, we set $T_2 = 8T_1 = 40$ min, while if the disturbance is inactive, we set $T_2 = T_1 = 5$ min.

For the IEEE 118-bus system, we assume the system is initially operating at the optimal power flow solution at $129627/hour. A disturbance takes line 23-24 out of service and the SSV drops to 0.1534, which we assume is below the stability margin threshold. We assume all load at PQ buses is responsive (1197 MW out a total of 4242 MW of system-wide demand) and set $\alpha = 10000$. Whether or not the disturbance is active, $T_2 = T_1 = 5$ min.

All computations are implemented in MATLAB on an Intel(R) i5-6600K CPU with 8 GB of RAM.

A. IEEE 9-Bus System Results

Figures 3 and 4 show the loading pattern, SSV, generation dispatch, and generation cost per hour in each period. In Fig. 3, we distinguish between SSVs when the disturbance is active and inactive – SSVs denoted with white circles (active) are comparable, SSVs denoted with black circles (inactive) are comparable, but SSVs denoted with white circles are not comparable to those denoted with black circles. In Period 1, the SSV increases by 6.1% due to the DR actions. Note that generation, with the exception of the slack bus, is constant in Periods 0 and 1. Next, we pay back the energy in Period 2. If the disturbance is still active, we maintain the SSV and the generation cost per hour is relatively large, whereas if the disturbance is inactive, the SSV increases due to the change in system topology. The cost per hour is comparable to that in the other periods. The actual generation cost of Period 2 is the cost per hour multiplied by the length of the period, and since T_2 with an active disturbance is much larger than T_2 without, the actual cost difference between the two cases is more extreme than it appears in the figure.

Figure 5 shows the SSV in Period 1 and the generation cost in Period 2 as α varies in the case with an active disturbance in Period 2. The weighting factor trades the stability margin improvement for generation cost reduction, and the best choice

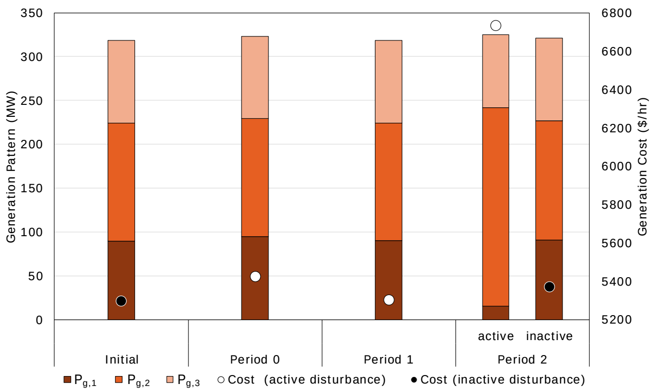

Fig. 4. Generation dispatch and generation cost per hour in each period for the IEEE 9-bus system.

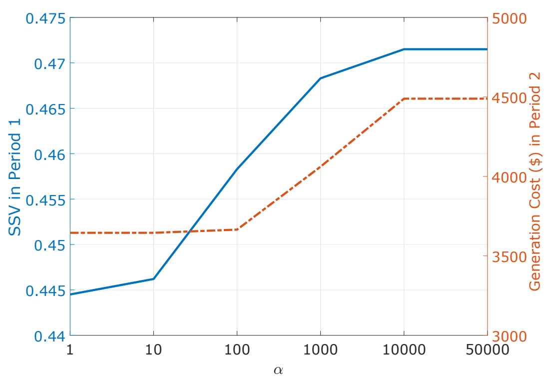

Fig. 5. Optimal SSV in Period 1 and generation cost in Period 2 as a function of the weighting factor α.

of α for a particular system is based on operator priorities. For this system, the SSV in Period 1 is maximized when $\alpha \geq 10000$. However, the impact of this parameter is system-dependent.

B. IEEE 118-Bus System Results

Figure 6 shows the SSV and generation cost per hour in each period. The SSV increases by 7.3% due to the DR actions in Period 1. Again, we show two cases in Period 2 and, again, the SSV is higher (due to the change in system topology) and the generation cost is lower if the disturbance is inactive.

Figure 7 visualizes the DR actions in Period 1. Red shading in the upper semicircle corresponding to a bus denotes an increase in load, while blue shading in the lower semicircle denotes a decrease in load. The lightning symbol indicates the line removed from service by the disturbance. In this case, the SSV is improved by decreasing the loading in Area 1 and increasing the loading in Area 2.

C. Comparison of Cases

We compare seven cases with different decision variables and/or parameters to the base case in Table I, which defines each case and shows its optimal SSV, percent improvement, and generation cost. For this comparison, we use the IEEE 9-bus system and only solve the first period problem.

Case 1 corresponds to our base case. Case 2 uses the loads rather than the slack bus to compensate for the change in

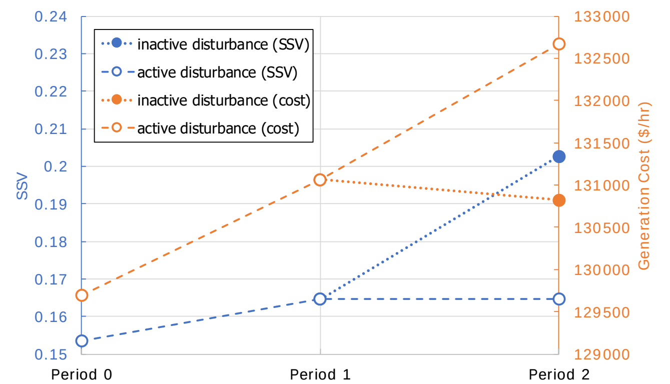

Fig. 6. SSV and generation cost per hour in each period for the 118-bus system.

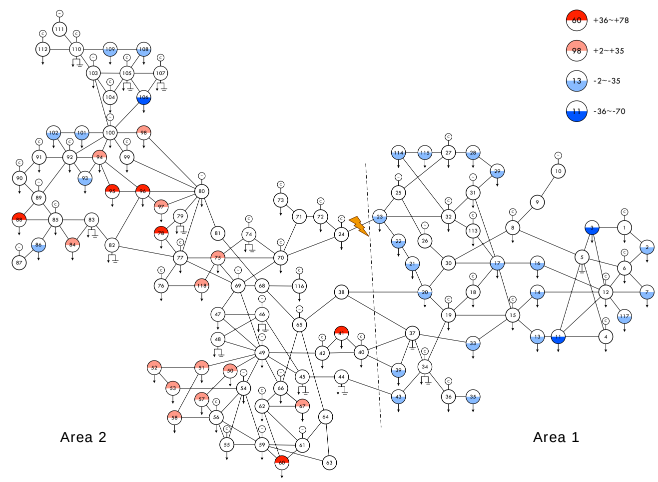

Fig. 7. Visualization of the DR actions in Period 1 for the IEEE 118-bus system. Figure created with the help of [39].

system losses. The total loading increases from 315 MW to 319 MW, reducing the optimal SSV slightly. In Cases 3–6, we investigate the achievable change in SSV using generator actions alone (in these cases, ε is irrelevant because there is no DR). The improvement possible through changes to generator real power generation (Case 3) is slightly greater than that of the base case (6.5% vs. 6.1%), but at a significantly higher generation cost. In Case 4, Generators 2 and 3 are modeled as steam turbine plants with 3 MW/minute (1% of capacity [40]) ramp rates, which reduces their ability to respond and the achievable SSV. Case 5 allows real power generation and voltage magnitudes to change. Voltage regulation alone (Case 6) does not improve the SSV very much. The greatest SSV improvement is achieved when we change load, generation, and voltage magnitudes together (Case 7); however, in practice, generators are ramp limited and so we would expect a realistic achievable improvement between that obtained in Case 7 and Case 8, where we have applied the conservative ramp rate used in Case 4.

The generation costs shown in the table are the costs per hour of Period 1 only; the next subsection describes the cost results of the multiperiod problem. The relative costs of the cases are system dependent; however, assuming that the system is initially dispatched at minimum cost, DR actions

TABLE I
DECISION VARIABLES, PARAMETERS, OPTIMAL SSV, PERCENT IMPROVEMENT, AND GENERATION COST FOR EACH CASE

Case	1	2	3	4	5	6	7	8
$P_{\mathrm{g,ref}}$	✓		✓	✓	✓		✓	✓
$P_{\mathrm{g},n} \forall n \in \mathcal{S}_{\mathrm{PV}}$			✓	✓	✓		✓	✓
$V_n \forall n \in \mathcal{S}_{\mathrm{G}}$					✓	✓	✓	✓
$P_{\mathrm{d},n}$, $Q_{\mathrm{d},n} \forall n \in \mathcal{S}_{\mathrm{DR}}$	✓	✓					✓	✓
1% Ramp Rate				✓				✓
ε	0	1	N/A	N/A	N/A	N/A	0	0
Optimal SSV	0.4715	0.4703	0.4732	0.4569	0.4783	0.4469	0.4885	0.4802
Percent improvement	6.1	5.8	6.5	2.3	7.6	0.5	9.9	8.0
Generation cost ($/hr)	5304.6	5424.5	8270.4	5501.6	8502.6	5424.5	7107.8	5428.1

TABLE II
COST OVER ONE HOUR ($) OF THE MULTIPERIOD DR STRATEGY VERSUS GENERATION REDISPATCH TO ACHIEVE THE SAME SSVS

T_{restored}	Resource	9-bus	118-bus
5 min	DR	5303	129545
	Generation	5360	129905
1 hour	DR	6441	132777
	Generation	6043	132961

will be less expensive than generator actions in Period 1.

We also formulated and solved an optimization problem to determine the minimum load shedding needed to achieve the same SSV improvement as obtained in Case 1 (without system-wide load shedding). The formulation is as follows.

$$\min \sum_{i\in\mathcal{S}_{\mathrm{DR}}} P_{d,i}(0) - \sum_{i\in\mathcal{S}_{\mathrm{DR}}} P_{d,i}(1) \tag{10a}$$

$$\sigma_0(1) = \sigma_{\min}\{J(\boldsymbol{\theta(1)}, \boldsymbol{V(1)})\} \tag{10b}$$

$$\mathcal{F}_n^P(\boldsymbol{\theta(1)}, \boldsymbol{V(1)}) = P_{g,n}(1) - P_{d,n}(1) \qquad \forall n \in \mathcal{N} \tag{10c}$$

$$\mathcal{F}_n^Q(\boldsymbol{\theta(1)}, \boldsymbol{V(1)}) = Q_{g,n}(1) - Q_{d,n}(1) \qquad \forall n \in \mathcal{N} \tag{10d}$$

$$P_{g,n}(1) = P_{g,n}(0) \qquad \forall n \in \mathcal{S}_{\mathrm{PV}} \tag{10e}$$

$$\sigma_0(1) \geq 0.4715 \tag{10f}$$

$$\underline{P}_{g,\mathrm{ref}}(1) \leq P_{g,\mathrm{ref}}(1) \leq \overline{P}_{g,\mathrm{ref}}(1) \tag{10g}$$

$$\underline{Q}_{g,n}(1) \leq Q_{g,n}(1) \leq \overline{Q}_{g,n}(1) \qquad \forall n \in \mathcal{S}_{\mathrm{G}} \tag{10h}$$

$$\underline{V}_n(1) \leq V_n(1) \leq \overline{V}_n(1) \qquad \forall n \in \mathcal{S}_{\mathrm{DR}} \tag{10i}$$

To solve this problem, we again use iterative linear programming with singular value sensitivities. In [11], the authors formulate a similar problem and also use singular value sensitivities to formulate a linear program. However, they only solve the linear program once and so the solution they obtain does not necessarily satisfy the original problem's constraints. By solving (10), we found that the system load would need to drop by at least 17% to achieve the same stability margin improvement as achieved by spatio-temporal load shifting. Load shedding has significant financial and comfort impacts for consumers.

D. Comparison of Costs

Table II summarizes the cost over one hour of the multiperiod DR strategy (with Period 1 decision variables corresponding to Case 1) for different disturbance restoration times T_{restored}. It also compares the results to the minimum-cost redispatch of generation alone (corresponding to the decision variables in Case 5, i.e., the generators are not limited by ramp rates) to achieve the SSV obtained using DR alone. The cost of each period is computed as the cost per hour times the length of the period, where all periods are 5 min except for the 9-bus system's Period 2 when the disturbance is active, which is 40 minutes (As a reminder, 40 minutes was chosen since it is the shortest multiple of 5 minutes for which we can obtain a feasible solution.) When $T_{\text{restored}} = 5$ min, the cost per hour of operating the system beyond Periods 1 and 2 but within the hour is equal to the cost per hour of Period 0. However, when $T_{\text{restored}} = 1$ hr, this cost is equal to the cost of using the generators to maintain the SSV achieved in Periods 1 and 2.

As shown in the table, the cost of the strategy increases as T_{restored} increases. Comparing the cost of using DR versus generation, we see that the cheaper option is case dependent. In three out of the four cases, DR is cheaper; however, when $T_{\text{restored}} = 1$ hour, generation actions are cheaper than DR actions for the 9-bus system. As described in the previous subsection, DR is always cheaper in Period 1. However, energy payback in Period 2 can be expensive, which is true for the 9-bus system when the disturbance is active, as shown in Fig. 4. Moreover, in this case, Period 2 lasts for 40 min.

Note that the generation costs reported in the table may not be realizable in practice because real generators are ramp-limited. Therefore, in cases in which DR is more expensive then generation, it may still be desirable to deploy DR since generation may not respond in time.

E. Comparison of Algorithms

In this subsection, we compare the performance of the ILP and INLP algorithms. Table III shows the optimal loading pattern and SSV computed using each algorithm for the IEEE 9-bus system considering only Period 1. The solutions/SSVs produced by the algorithms are close. Figure 8 shows the convergence of each algorithm on the 9-bus system considering the full multiperiod problem (disturbance active in Period 2). The solid lines are the results of the ILP algorithm and the dashed lines are the results of the INLP algorithm. The ILP algorithm converges more quickly than the INLP algorithm. Similarly, Fig. 9 shows the convergence of the ILP algorithm on the 118-bus system considering the full multiperiod problem (disturbance active in Period 2). The INLP algorithm does not scale to the 118-bus system.

The computation times are summarized in Table IV. In addition to ILP and INLP, we also show the computation times for the eigenvalue sensitivity approach from our previous work [15], referred to as ILP-E. As shown, the ILP algorithm requires significantly less time than the INLP algorithm, and roughly half as much time as ILP-E. The overall computation time is a function of the number of iterations needed and the time required for each iteration, where the former depends on the initial operating point and the maximum step size $\overline{\Delta\sigma_0}$ and the latter depends on the size of Jacobian matrix. The time could be reduced through 1) parallel computing of the SSV sensitivities, 2) approximating the SSV sensitivity (9b) to

TABLE III
LOADING PATTERN & SSV COMPUTED WITH ILP AND INLP FOR THE IEEE 9-BUS SYSTEM

Algorithm	Nominal	Optimal ILP	Optimal INLP
$P_{\mathrm{d},5}$ (MW)	90	147.93	149.58
$P_{\mathrm{d},7}$ (MW)	100	137.23	135.57
$P_{\mathrm{d},9}$ (MW)	125	29.84	29.85
SSV	0.4445	0.4715	0.4716

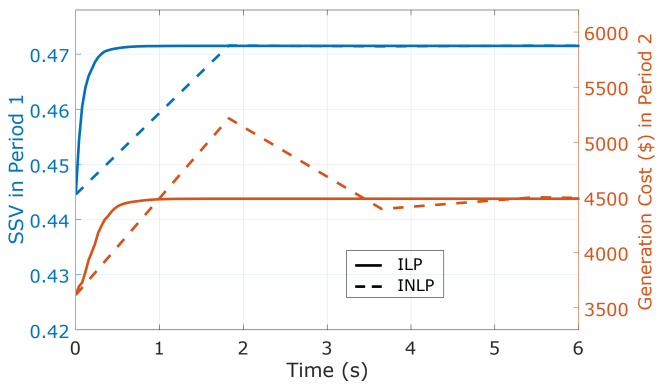

Fig. 8. Convergence of the SSV in Period 1 and the generation cost in Period 2 using the ILP and INLP algorithms for the IEEE 9-bus system.

only include the system states that most affect the SSV, and/or 3) applying an adaptive maximum step size.

V. Conclusion and Future Work

In this paper, we have developed a multiperiod optimal power flow approach to use DR to improve static voltage stability as measured by the smallest singular value of the power flow Jacobian matrix. In addition to formulating the problem, which increases/decreases loads while holding total load constant in a first period and paying back energy to each load in a second period, we have developed an iterative linear programming algorithm using singular value sensitivities. We demonstrated the performance of the approach on the IEEE 9- and 118-bus systems, compared the effectiveness and cost of DR actions to generation actions, and benchmarked our algorithm against an iterative nonlinear programming algorithm from the literature.

A primary drawback to using the SSV as a voltage stability metric is that it is an indicator of the distance to infeasibility of the power flow equations; it does not contain information about the distance to the engineering or security constraints. Future work will explore and/or develop alternative metrics that do include this information. Other avenues for future work include developing an understanding of why the loading patterns change in the way they do and improving the computational speed of our algorithm. Furthermore, we would like to improve the algorithm to explicitly consider the path between each operating point, ensuring an adequate voltage stability margin along the the path. For this, we could leverage ideas from [41]–[43]. Finally, we would like to develop formulations that incorporate other stability metrics and determine how different metrics impact the control of resources. For example, we have conducted a preliminary exploration of the potential for spatio-temporal load shifting to improve small signal stability [44].

TABLE IV
COMPUTATION TIMES (S)

	ILP	ILP-E	INLP
IEEE 9-bus system, Period 1 only	0.4	1.0	2.5
IEEE 9-bus system, Full problem	1.0	2.8	6.0
IEEE 118-bus system, Period 1 only	6.5	15	-
IEEE 118-bus system, Full problem	35	60	-

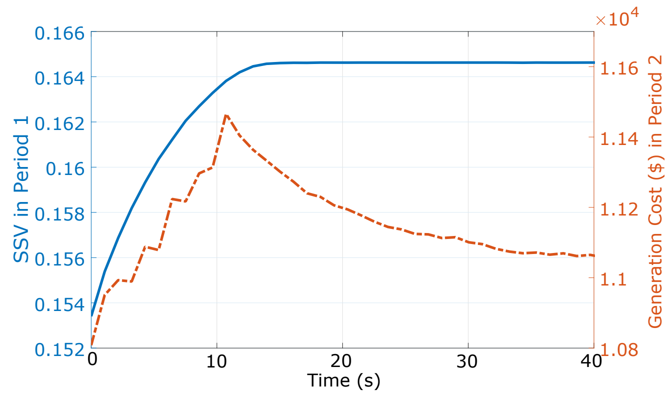

Fig. 9. Convergence of the SSV in Period 1 and the generation cost in Period 2 using the ILP algorithm for the IEEE 118-bus systems.

References

[1] S. Eftekharnejad, V. Vittal, G. T. Heydt, B. Keel, and J. Loehr, “Impact of increased penetration of photovoltaic generation on power systems,” *IEEE Transactions on Power Systems*, vol. 28, no. 2, pp. 893–901, 2013.

[2] A. Ulbig, T. S. Borsche, and G. Andersson, “Impact of low rotational inertia on power system stability and operation,” *Proceedings of IFAC*, vol. 47, no. 3, pp. 7290–7297, 2014.

[3] S. Greene, I. Dobson, and F. L. Alvarado, “Sensitivity of the loading margin to voltage collapse with respect to arbitrary parameters,” *IEEE Transactions on Power Systems*, vol. 12, no. 1, pp. 262–272, 1997.

[4] R. Al Abri, E. F. El-Saadany, and Y. M. Atwa, “Optimal placement and sizing method to improve the voltage stability margin in a distribution system using distributed generation,” *IEEE Transactions on Power Systems*, vol. 28, no. 1, pp. 326–334, 2013.

[5] M. El-Sadek, M. Dessouky, G. Mahmoud, and W. Rashed, “Enhancement of steady-state voltage stability by static var compensators,” *Electric Power Systems Research*, vol. 43, no. 3, pp. 179–185, 1997.

[6] J. Short, D. Infield, and L. Freris, “Stabilization of grid frequency through dynamic demand control,” *IEEE Transactions on Power Systems*, vol. 22, no. 3, pp. 1284–1293, 2007.

[7] D. Callaway, “Tapping the energy storage potential in electric loads to deliver load following and regulation, with application to wind energy,” *Energy Conversion and Management*, vol. 50, pp. 1389–1400, 2009.

[8] W. Zhang, J. Lian, C.-Y. Chang, and K. Kalsi, “Aggregated modeling and control of air conditioning loads for demand response,” *IEEE Transactions on Power Systems*, vol. 28, no. 4, pp. 4655–4664, 2013.

[9] D. S. Callaway and I. A. Hiskens, “Achieving controllability of electric loads,” *Proceedings of the IEEE*, vol. 99, no. 1, pp. 184–199, 2011.

[10] Z. Feng, V. Ajjarapu, and D. J. Maratukulam, “A practical minimum load shedding strategy to mitigate voltage collapse,” *IEEE Transactions on Power Systems*, vol. 13, no. 4, pp. 1285–1290, 1998.

[11] A. Berizzi, P. Bresesti, P. Marannino, G. Granelli, and M. Montagna, “System-area operating margin assessment and security enhancement against voltage collapse,” *IEEE Transactions on Power Systems*, vol. 11, no. 3, pp. 1451–1462, 1996.

[12] Y. Yu, L. Liu, K. Pei, H. Li, Y. Shen, and W. Sun, “An under voltage load shedding optimization method based on the online voltage stability analysis,” in *Proceedings of IEEE POWERCON*, 2016.

[13] G. Irisarri, X. Wang, J. Tong, and S. Mokhtari, “Maximum loadability of power systems using interior point nonlinear optimization method,” *IEEE Transactions on Power Systems*, vol. 12, no. 1, pp. 162–172, 1997.

[14] R. J. Avalos, C. A. Cañizares, F. Milano, and A. J. Conejo, "Equivalency of continuation and optimization methods to determine saddle-node and limit-induced bifurcations in power systems," *IEEE Transactions on Circuits and Systems I: Regular Papers*, vol. 56, no. 1, pp. 210–223, 2009.
[15] M. Yao, J. L. Mathieu, and D. K. Molzahn, "Using demand response to improve power system voltage stability margins," in *Proceedings of IEEE PowerTech, Manchester*, 2017.
[16] I. Dobson and L. Lu, "Computing an optimum direction in control space to avoid stable node bifurcation and voltage collapse in electric power systems," *IEEE Transactions on Automatic Control*, vol. 37, no. 10, pp. 1616–1620, 1992.
[17] I. Dobson, "Distance to bifurcation in multidimensional parameter space: Margin sensitivity and closest bifurcations," *Bifurcation Control*, pp. 704–706, 2003.
[18] M. Yao, I. A. Hisken, and J. L. Mathieu, "Improving power system voltage stability by using demand response to maximize the distance to the closest saddle-node bifurcation," in *Proceedings of 57th IEEE Conference on Decision and Control (CDC)*, 2018.
[19] R. J. Thomas and A. Tiranuchit, "Voltage instabilities in electric power networks," in *Proceedings of 18th Southeast Symposium on System Theory*, 1986, pp. 359–363.
[20] A. Berizzi, P. Finazzi, D. Dosi, P. Marannino, and S. Corsi, "First and second order methods for voltage collapse assessment and security enhancement," *IEEE Transactions on Power Systems*, vol. 13, no. 2, pp. 543–551, 1998.
[21] A. Berizzi, Y.-G. Zeng, P. Marannino, A. Vaccarini, and P. A. Scarpellini, "A second order method for contingency severity assessment with respect to voltage collapse," *IEEE Transactions on Power Systems*, vol. 15, no. 1, pp. 81–87, 2000.
[22] A. Tiranuchit and R. Thomas, "A posturing strategy against voltage instabilities in electric power systems," *IEEE Transactions on Power Systems*, vol. 3, no. 1, pp. 87–93, 1988.
[23] A. Tiranuchit, L. Ewerbring, R. Duryea, R. Thomas, and F. Luk, "Towards a computationally feasible on-line voltage instability index," *IEEE Transactions on Power Systems*, vol. 3, no. 2, pp. 669–675, 1988.
[24] P.-A. Lof, T. Smed, G. Andersson, and D. Hill, "Fast calculation of a voltage stability index," *IEEE Transactions on Power Systems*, vol. 7, no. 1, pp. 54–64, 1992.
[25] E. Mallada and A. Tang, "Dynamics-aware optimal power flow," in *Proceedings of 52nd IEEE Conference on Decision and Control (CDC)*, 2013, pp. 1646–1652.
[26] I. A. Hiskens and R. J. Davy, "Exploring the power flow solution space boundary," *IEEE Transactions on Power Systems*, vol. 16, no. 3, pp. 389–395, 2001.
[27] C. Cañizares, W. Rosehart, A. Berizzi, and C. Bovo, "Comparison of voltage security constrained optimal power flow techniques," in *Proceedings of IEEE PES Summer Meeting*, vol. 3, 2001, pp. 1680–1685.
[28] R. J. Avalos, C. A. Cañizares, and M. F. Anjos, "A practical voltage-stability-constrained optimal power flow," in *Proceedings of IEEE PES General Meeting*, 2008.
[29] W. Rosehart, C. Cañizares, and V. Quintana, "Optimal power flow incorporating voltage collapse constraints," in *Proceedings of IEEE PES Summer Meeting*, vol. 2, 1999, pp. 820–825.
[30] G. G. Lage, G. R. da Costa, and C. A. Cañizares, "Limitations of assigning general critical values to voltage stability indices in voltage-stability-constrained optimal power flows," in *Proceedings of IEEE POWERCON*, 2012.
[31] O. A. Urquidez and L. Xie, "Singular value sensitivity based optimal control of embedded VSC-HVDC for steady-state voltage stability enhancement," *IEEE Transactions on Power Systems*, vol. 31, no. 1, pp. 216–225, 2016.
[32] M. Yao, D. K. Molzahn, and J. L. Mathieu, "The impact of load models in an algorithm for improving voltage stability via demand response," in *Proceedings of Allerton Conference on Communication, Control, and Computing*, 2017.
[33] A. J. Wood and B. F. Wollenberg, *Power Generation, Operation, and Control*. John Wiley & Sons, 2012.
[34] S. K. Kodsi and C. A. Cañizares, "Application of a stability-constrained optimal power flow to tuning of oscillation controls in competitive electricity markets," *IEEE Transactions on Power Systems*, vol. 22, no. 4, pp. 1944–1954, 2007.
[35] J. Lavaei and S. H. Low, "Zero duality gap in optimal power flow problem," *IEEE Transactions on Power Systems*, vol. 27, no. 1, pp. 92–107, 2012.
[36] D. K. Molzahn and I. A. Hiskens, "Convex relaxations of optimal power flow problems: An illustrative example," *IEEE Transactions on Circuits and Systems I: Regular Papers*, vol. 63, no. 5, pp. 650–660, 2016.
[37] J. F. Marley, D. K. Molzahn, and I. A. Hiskens, "Solving multiperiod OPF problems using an AC-QP algorithm initialized with an SOCP relaxation," *IEEE Transactions on Power Systems*, vol. 32, no. 5, pp. 3538–3548, 2017.
[38] R. Zimmerman, C. Murillo-Sanchez, and R. Thomas, "MATPOWER: Steady-state operations, planning, and analysis tools for power systems research and education," *IEEE Transactions on Power Systems*, vol. 26, no. 1, pp. 12–19, Feb 2011.
[39] NICTA/Monash University, *Steady-State AC Network Visualization in the Browser*. [Online]. Available: http://immersive.erc.monash.edu.au/stac/
[40] V. Vittal, J. McCalley, V. Ajjarapu, and U. V. Shanbhag, "Impact of increased DFIG wind penetration on power systems and markets," Power Systems Engineering Research Center (PSERC), Tech. Rep. 09-10, 2009.
[41] R. Pedersen, C. Sloth, and R. Wisniewski, "Verification of power grid voltage constraint satisfactiona barrier certificate approach," in *Proceedings of the 2016 European Control Conference (ECC)*. IEEE, 2016, pp. 447–452.
[42] I. A. Hiskens and M. Pai, "Trajectory sensitivity analysis of hybrid systems," *IEEE Transactions on Circuits and Systems I, Fundamental Theory and Applications*, vol. 47, no. 2, pp. 204–220, 2000.
[43] T. B. Nguyen and M. Pai, "Dynamic security-constrained rescheduling of power systems using trajectory sensitivities," *IEEE Transactions on Power Systems*, vol. 18, no. 2, pp. 848–854, 2003.
[44] K. Koorehdavoudi, M. Yao, J. L. Mathieu, and S. Roy, "Using demand response to shape the fast dynamics of the bulk power network," in *Proceedings of IREP Symposium on Bulk Power System Dynamics and Control, Espinho, Portugal*, 2017.

Mengqi Yao (S'17) received the B.S. degree in electric power engineering and automation from Shanghai Jiao Tong University, Shanghai, China, in 2014 and the M.S. degree in electrical engineering: systems from the University of Michigan, Ann Arbor, MI, USA, in 2016, where she is currently pursuing the Ph.D. degree in electrical engineering. Her research interests include developing strategies to control distributed energy resources to improve power system stability and power quality.

Daniel K. Molzahn (S'09-M'13) is an Assistant Professor in the School of Electrical and Computer Engineering at the Georgia Institute of Technology and also holds an appointment as a computational engineer in the Energy Systems Division at Argonne National Laboratory. He was a Dow Postdoctoral Fellow in Sustainability at the University of Michigan, Ann Arbor. He received the B.S., M.S., and Ph.D. degrees in electrical engineering and the Masters of Public Affairs degree from the University of Wisconsin–Madison, where he was a National Science Foundation Graduate Research Fellow. His research focuses on optimization and control of electric power systems.

Johanna L. Mathieu (S'10-M'12-SM'18) received the B.S. degree in ocean engineering from the Massachusetts Institute of Technology, Cambridge, MA, USA, in 2004 and the M.S. and Ph.D. degrees in mechanical engineering from the University of California, Berkeley, USA, in 2008 and 2012, respectively. She is an Assistant Professor in the Department of Electrical Engineering and Computer Science at the University of Michigan, Ann Arbor, MI, USA. Prior to joining the University of Michigan, she was a postdoctoral researcher at the Swiss Federal Institute of Technology (ETH) Zurich, Switzerland. Her research interests include modeling, estimation, control, and optimization of distributed energy resources.